Theoret. Chim. Acta (Berl.) 48, 1–15 (1978)

THEORETICA CHIMICA ACTA
© by Springer-Verlag 1978

Original Investigations

Simple *ab initio* Calculations Using a Floating Basis

The Electronic Structure and Properties of the Rotamers of Hydrogen Disulphide

Peter H. Blustin

Department of Chemistry, The University, Sheffield S3 7HF, United Kingdom

Calculations are described on three rotamers of hydrogen disulphide (*trans*-, *gauche*- and *cis*-HSSH) using an *ab initio* Floating Gaussian Orbital model. The optimised geometrical and electronic structures of each rotamer are discussed in terms of several electronic properties, a population and orbital analysis and an extensive partitioning of the electronic energy amongst the orbitals. The so-called Gauche Effect in HSSH is discussed in connexion with the various models proposed to account for this particular structural feature.

Key words: Hydrogen disulphide – Floating Gaussian orbital calculations

1. Introduction

There seem to be two reasons why the adoption of the gauche conformation by hydrogen disulphide is unexpected. Firstly, perhaps on intuitive grounds, because nonbonded interactions across the molecule should lead to *trans*-HSSH being the most stable. Secondly, because the lowest energy configuration of its fluorine analogue has the gas phase structure $S{=}SF_2$ [1]. The system $S{=}SH_2$ has never been observed, although it was thought at one time to be the actual structure of hydrogen disulphide [2].

The gauche conformation is of course a common structural feature in catenated Group VIa and in many other molecular systems. The origin of the so-called Gauche Effect has been much discussed, and it has been pointed out that the proximity of adjacent lone pairs and polar bonds is a characteristic of this structural conformation [3]. In the present article, the results of calculations on *cis*-, *trans*- and *gauche*-HSSH will be considered in connexion with the several electronic mechanisms advanced to account for the observed structure of this molecule.

0040–5744/78/0048/0001/$03.00

2. Theory and Calculations

The calculations were made according to an adaption of Frost's *ab initio* Floating Spherical Gaussian Orbital (FSGO) model [4]. This approach assumes that the electronic structure of a particular molecule may be described by a single Slater determinant of doubly-occupied nonorthogonal spherical Gaussian functions,

$$\psi = \mathcal{A} G_1(1)\,\overline{G_1(2)} \ldots G_n(2n-1)\,\overline{G_n(2n)}$$

in which $G_i(r) = [2\alpha_i/\pi]^{3/4} \exp[-\alpha_i(r-R_i)^2]$ is an FSGO with exponent α_i, centred at R_i. The variational energy of this Slater determinant is minimized by varying the position and exponent of each orbital function.

The present calculations utilized a combination of floating *s*-type and *p*-type lobe Gaussian functions (Floating Gaussian Orbitals – FGO), which is described elsewhere [5]. The orbital configuration for the gauche conformer is illustrated in Fig. 1. Each sulphur *KL* inner core is represented by a "conventional" atomic

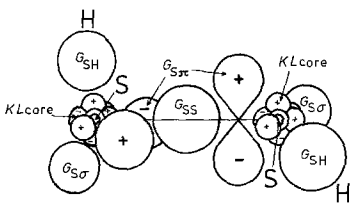

Fig. 1. FGO configuration for gauche-HSSH (schematic)

$G_{1s}G_{2s}G_{2p_x}G_{2p_y}G_{2p_z}$ arrangement. S–S and S–H bonding orbitals, G_{SS} and G_{SH} and the σ nonbonding orbitals on the sulphurs, $G_{S\sigma}$, were unconstrained except by symmetry. The nonbonding orbitals of π-symmetry, $G_{S\pi}$, however, could only move in the plane perpendicular to the *p*-type function. Certain orbitals were given common exponents, so that they were optimised in groups $-\alpha_{1s}$; $\alpha_{2s,2p}$; α_{SS}; α_{SH}; $\alpha_{S\sigma,\pi}$.

3. Results

3.1. Energies

The computed total and partitioned molecular energies of *gauche*-HSSH are given in Table 1, together with changes calculated for the *trans* and *cis* rotamers. Table 2 lists values of the rotational barriers in HSSH taken from the present and from other sources [6–15]. The energy changes listed in Table 1 are clearly dominated by the nucleus-electron attraction energy. It is the maximization of this energy which discriminates between the rotamers, giving the lowest energy *gauche*-HSSH the most compact structure, in which all the other (repulsive) energies are *also* at a maximum [16–18].

Values of the *trans* and *cis* barriers given in Table 2 have been obtained by several methods. The experimental estimate of the HSSH barriers by Winnewisser *et al.*

Table 1. Partitioned energies and energy differences (in a.u.[a]) calculated for the rotamers

	cis-HSSH $\xleftarrow{\Delta}$	*gauche*-HSSH $\xrightarrow{\Delta}$	*trans*-HSSH
Nucleus-electron attraction	+2.140900	−1839.982803	+1.118038
Electron-electron repulsion	−1.052465	+375.819533	−0.559448
Electronic kinetic energy	−0.019643	+686.742321	−0.015724
Electronic energy	+1.068793	−777.420949	+0.542866
Nucleus-nucleus repulsion	−1.048553	+90.678635	−0.530728
Total molecular energy	+0.020240	−686.742314	+0.012138

[a] 1 a.u. = 2625.5637 kJ mol^{-1}.

[14] was that they were approximately equal, appreciably greater than in HOOH and not less than 24 kJ mol^{-1}. Allinger *et al.* [15] consider, from results obtained for substituted disulphides and from other sources, that the *trans* barrier is about 29 kJ mol^{-1}, the *cis* being about 45% higher at about 42 kJ mol^{-1}. The only calculations to be in accord with this empirical estimate are those of Veillard and Demuynck [7] (*cis* 55% higher than *trans*) and the FGO results described herein (66%). The former calculation used the best quality basis set and would be the most reliable one if they had included geometry optimization. The FGO calculations were the only ones to perform a complete geometry variation. The relatively high FGO values may be due to the comparatively short S–S bond (see below) leading to greater interactions across the molecule.

Table 2. Calculated and empirical rotational barriers (kJ mol^{-1})

Method	Basis	Reference	Geometry varied[a]	*trans*	*cis*
ab initio (1969)	S(10, 6), H(3)	[6]	fixed	7.9	33.3
ab initio (1969)	S(12, 9, 1), H(5, 1)	[7]	fixed	25.1	39.0
ab initio (1970)	S(11, 6), H(4)	[8]	fixed	9.4	32.3
ab initio (1973)	FGO–SCF	[9]	r_{ss}	14.2	36.8
CNDO (1974)		[10]	r_{ss}	15.1	45.6
ab initio (1974)	S(12, 9, 1), H(4, 1)	[11]	fixed	17.9	34.4
Pseudopotential (1975)		[12]	fixed	4.8	33.5
ab initio (1976)	S(10, 6, 1), H(4, 1)	[13]	fixed	17.6	35.2
ab initio (1977)	FGO	this work	all parameters	31.9	53.1
Experimental estimate (1968)		[14]		>24	>24
Empirical estimate (1976)		[15]		~29	~42

[a] Excluding dihedral angle.

3.2. Geometries

The results obtained for the optimum geometry of each system investigated are given in Table 3, along with experimental results [14]. A direct comparison of

Table 3. Geometries[a]

	r_{SS}	r_{SH}	SSH	θ_d
cis-HSSH	1.953	1.297	94.8	0
gauche-HSSH[b]	1.922	1.298	95.9	90.7
trans-HSSH	1.937	1.304	92.9	180

[a] r_e values in Å, angles in degrees.
[b] Experiment [14] $r_{SS}=2.055$ Å, $r_{SH}=1.327$ Å, $\widehat{SSH}=91.3°$, $\theta_d=90.6°$.

theoretical r_e and θ_e values with experimental r_0 and θ_0 results is not strictly possible, however, discrepancies are not too large – about 2% in S–H distances, 6% in r_{SS} and less than 3% in angles.

The calculations imply that the S–H bond lengthens on the dimerization of the SH radical ($r_{SH}=1.294$Å [19]) to form HSSH. Rotation from *gauche-* to *cis*-HSSH brings about a slight decrease in r_{SH}. The S–S bond is shortest in the lowest energy rotamer and is inversely proportional to the relative energies of the rotamers.

Angle changes on rotation seem to be dominated by the interactions between the lone pairs. Figure 2 shows how the valence electron pair interactions about each

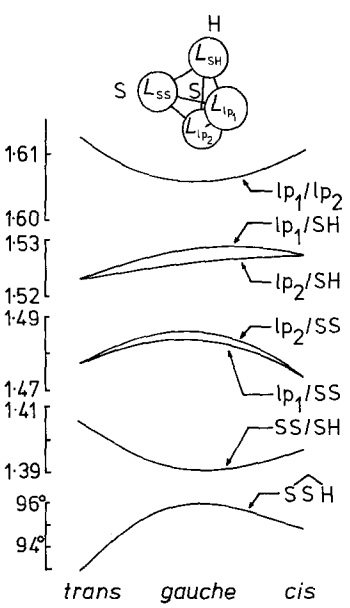

Fig. 2. Rotational changes in VSEPR interactions (a.u.) about each sulphur centre (not to scale)

sulphur centre change on rotation (the interaction is defined by – see Sect. 4.1. – $pr_A/pr_B = 2[2\langle pr_A pr_A|h_2|pr_B pr_B\rangle - \langle pr_A pr_B|h_2|pr_B pr_A\rangle]$, h_2 = two-electron operator). The interactions increase in the order $bp/bp < bp/lp < lp/lp$, as required by Valence Shell Electron Pair Repulsion (VSEPR) theory [20]. The SSH angle changes according to the sequence *trans* < *cis* < *gauche*, which parallels the changes in lp_1/lp_2, but *in reverse*. In the *gauche* rotamer, the lone pairs seem to be most delocalized (see later discussion), so that lp_1/lp_2 is at its lowest value. For the *cis* and *trans* rotamers, lp_1/lp_2 follows the trend in the repulsive energies – see Table 1 – mentioned above.

3.3. Electronic Properties

Table 4 lists the results obtained for a series of first and second order properties of the molecules under investigation [19]. The calculated dipole moments for

Table 4. First and second order properties

Property	*trans*-HSSH	*gauche*-HSSH	*cis*-HSSH
μ_D[a]	0.0	0.882	1.327
$\Theta_B^{\alpha\alpha}$[b,f]	−7.493	−0.894	−7.453
$\Theta_B^{\beta\beta}$	+7.615	−2.334	+6.105
$\Theta_B^{\gamma\gamma}$	−0.122	+3.228	+1.347
$\chi_d^{\alpha\alpha}$[c,f]	−197.6	−192.0	−200.3
$\chi_d^{\beta\beta}$	−190.5	−192.0	−193.3
$\chi_d^{\gamma\gamma}$	−30.87	−30.66	−30.81
$\langle r^2\rangle$[c,f]	−139.6	−138.2	−141.5
$\langle 1/r_S\rangle_{total}$[d]	−51.775	−51.776	−51.775
$\langle 1/r_H\rangle_{total}$	−0.888	−0.901	−0.885
χ_m[e]	−389.0	−387.8	−388.3
χ_d	−1389.7	−1375.7	−1408.0
χ_p	+1000.7	+987.8	+1019.7
α[g]	6.324	6.291	6.304

[a] In debyes (3.335641×10^{-30} C m).
[b] In buckinghams (3.335641×10^{-40} C m^2).
[c] In a.u.^{2} (2.80018×10^{-21} m^2).
[d] In a.u.$^{-1}$ (3.02771×10^{-9} C m^{-1}).
[e] In 10^{-12} m^3 mol^{-1}.
[f] Calculated with respect to centre of mass (S = 33, H = 1).
[g] Average polarisability, in Å^3 (10^{-30} m^3).

gauche-HSSH and H_2S [21], 0.882 D and 0.789 D, are close to each other and compare well with the experimental results of 1.18 D [22] and 0.96 D [23], respectively. The directions of the overall moments corresponds to an S^-H^+ bond moment.

The diagonal elements of the quadrupole moment tensors (Table 4) for the HSSH rotamers show that there is surprisingly little change in the shape of the electron

density distribution on rotation, despite the conformational changes. The orientation of the principal axis system changes slightly on rotation, as expected. Θ_B^{zz} is related to the separation of charge brought about by the changing S–S internuclear distance, whereas the positive quadrupoles associated with the nonbonding S_π orbitals, Θ_B^{xx}, are counterbalanced by the S_σ and S–H combinations of π-symmetry, Θ_B^{yy}.

The principal axes of the diamagnetic susceptibility tensors χ_d coincide almost precisely with those of the quadrupoles (χ_d excludes the nuclear framework). The low absolute value of χ_d^{zz} in HSSH is related to the more tightly-bound σ-orbitals, whereas the more magnetically susceptible (or polarisable) π-orbital combinations of lone pair and S–H bonding orbitals give considerably larger values of χ_d^{xx} and χ_d^{yy}. Nevertheless, for this property, the average susceptibility of the π-orbital combinations in *gauche*-HSSH is less than in the *cis* or *trans* rotamers, despite the greater delocalization of the π-orbitals in the former rotamer (see next section).

That the electronic distribution in the *gauche* rotamer is the most compact is indicated by the values calculated for $\langle r^2 \rangle$ (which is proportional to the total average diamagnetic susceptibility, χ_d). This expectation value is related to the size or extent of the charge distribution, calculated with respect to the appropriate centre of mass. The trend *gauche* → *trans* → *cis* in $\langle r^2 \rangle$ follows the relative energies of the three systems.

The (temperature-independent) molar susceptibility χ_m may be calculated using Amos and Crispin's expressions [24]. It includes the diamagnetic term χ_d, already discussed, and a paramagnetic term χ_p. Since χ_m is nearly constant for the three rotamers, the paramagnetism is roughly proportional to the diamagnetism. The calculations therefore predict that there should be slight fluctuations, dependent upon temperature, in the so-called "temperature-independent" part of the susceptibility. This effect should be capable of detection at the present time [25].

The total potential experienced by a bonding electron pair, which changes slightly on rotation, depends upon the local nuclear plus electronic environment. For example, for the SS bonding orbital, the total potential at the orbital centre $\langle 1/r_{SS} \rangle_t$ may be written as

$$\langle 1/r_{SS} \rangle_t = 2\left(\frac{Z_S^{eff}}{r_{S/SS}} + \frac{1}{r_{H/SS}}\right) + 2P_{SH} + P_{SS}$$

The first two terms, in parentheses, represent the potential at this point due to the two sulphur nuclei screened by the core and nonbonding electrons (thus giving an effective charge Z_S^{eff}) and that due to the hydrogen nuclei ($Z=1$). The third and fourth terms are the contributions to $\langle 1/r_{SS} \rangle_t$ from the electron pairs of the SH bonding orbitals and the two electrons in the SS orbital itself. A similar expression may be deduced for $\langle 1/r_{SH} \rangle_t$; in this case, a slightly different value of Z_S^{eff} is required. The effective charges on the sulphur atoms, obtained by the solutions of these equations for Z_S^{eff}, show how the screening due to the nonbonding electrons changes on rotation (Table 5).

Table 5. Screening in HSSH

	Z_{SH}^{eff}	Z_{SS}^{eff}	$Z_{average}^{eff}$
cis-HSSH	3.152642	3.080150	3.116396
trans-HSSH	3.101336	3.094880	3.098108
gauche-HSSH	3.112991	3.080125	3.096558

Firstly, however, if the screening efficiency of the electrons in the sulphur K and L shells is virtually 100%, then it may be deduced that the nonbonding orbitals are only about 73% efficient (percent screening efficiency $= 100 \times (6 - Z_S^{eff})/4$, where 6 is the charge on S after 100% screening by core electrons, and 4 is the number of nonbonding electrons). The larger the value of Z_S^{eff}, the greater the attraction of the SH bonding orbital for the sulphur centre, and hence the shorter the S–H bond length. This inverse proportionality between $Z_S^{eff}(SH)$ and r_{SH} is obeyed on rotation. A similar effect holds for the *cis* and *trans* rotamers with respect to the S–S bond, that is, $Z_S^{eff}(SS)$ is inversely proportional to r_{SS}; however, for the *gauche* rotamer, the bonding between the sulphurs is rather different (see next section) since the π-orbitals have moved into a position between the SS orbital and the sulphur cores. This leads to greater screening of the sulphur nucleus by the (largely) nonbonding electrons. The third column in Table 5 shows that, on the average, the screening efficiency increases (Z_S^{eff} decreases) as the rotamer is stabilized. This may be connected both with the compactness of the distribution of electron density as well as with the disposition of the orbitals.

3.4. Population and Orbital Analysis

It is possible to perform a population analysis of FGO-type wavefunctions by the method of Simons and Talaty [26]. The results are given in Table 6, in which the σ and π contributions to the electronic populations are given separately [19]. Changes which take place on rotation from *gauche* to *cis*, or from *gauche* to *trans*, are all relatively small, rather less than calculated by Pappas [13]. The changes in the total populations imply that these rotations produce a slight net depletion of charge at S, which is then transferred to H. However, the sizes of the charge transfers are not proportional to the rotational barriers.

Table 6. Population analysis[a]

	trans-HSSH $\xleftarrow{\Delta}$	*gauche*-HSSH $\xrightarrow{\Delta}$	*cis*-HSSH
$N_\sigma(H)$	+0.001	1.192	−0.003
$N_\pi(H)$	+0.009	0.021	+0.004
$N(H)$	+0.010	1.213	+0.002
$N_\sigma(S)$	−0.001	13.808	+0.003
$N_\pi(S)$[b]	+0.013	1.957	+0.018
$N_\pi(S)$[c]	−0.022	0.022	−0.022
$N(S)$	−0.009	15.787	−0.002

[a] In electrons.
[b] With respect to S–H bond.
[c] With respect to S–S bond.

In the *gauche* orbital configuration, the nonbonding $G_{S\pi}$ orbitals move into the S–S region to produce a small π-orbital population of 0.022e at the opposite sulphur nucleus. This partial delocalization, or incipient triple bond [27], gives rise to the short S–S distance in this rotamer (Table 3). Rotation to the *cis* or *trans* conformer produces net reductions of 0.004e and 0.009e, respectively, in the π-electron population at the sulphurs.

It has been shown that the spherical nature of the FSGO's may be used to construct Packing Orbitals [28]. This has been carried out for HSSH in Table 7, using the diagram illustrated in Fig. 3. The three inter-orbital distances $r_{S/SS}$, $r_{S/SH}$ and

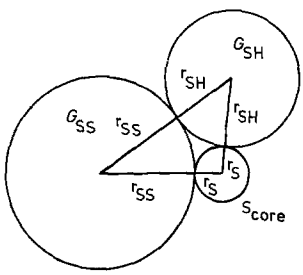

Fig. 3. Construction of Packing Orbitals for HSSH in the S/SS/SH environment

$r_{SS/SH}$ give three simultaneous equations which may be solved for the three unknowns, namely the radius of the core r_S and the radii of the S–S and S–H bonding orbitals, for example

$$r_S + r_{SS} = r_{S/SS}, \text{ etc.}$$

The positions of the lone pairs are taken to be the sum and difference of the $G_{S\sigma}$ and $G_{S\pi}$ orbital centres:

$$R_{\pm} = R_{\sigma} \pm R_{\pi}$$

The size of the lone pairs is then calculated with respect to the other valence orbitals, that is, G_{SS} and G_{SH}. The coincidence, or otherwise, obtained for r_{1p} through these two independent packing environments ($1p$/SS and $1p$/SH) gives an indication of how far the spherical nature of all the valence orbitals is retained for each rotamer. This is achieved (Table 7) best by *gauche*-HSSH. The 0.2% deviation in r_{1p} for this rotamer is easily comparable with results obtained for

Table 7. Packing orbital sizes (a.u.)

	trans-HSSH $\overset{\Delta}{\longleftarrow}$	*gauche*-HSSH $\overset{\Delta}{\longrightarrow}$	*cis*-HSSH
ψ_S	+0.0403 (+9.9%)	0.4087	+0.0166 (+4.1%)
ψ_{SS}	−0.0260 (−1.8%)	1.4076	+0.0123 (+0.9%)
ψ_{SH}	−0.0329 (−3.1%)	1.0541	−0.0222 (−2.1%)
ψ_{1p}	+0.0538[a] (+10.3%)	0.5199[b]	+0.0328[c] (+6.3%)

[a] 0.5737 ± 0.0132, or $\pm 2.3\%$.
[b] ± 0.0010, or $\pm 0.2\%$.
[c] 0.5527 ± 0.0077, or $\pm 1.4\%$.

ethane and disilane [28]. The conclusion to be drawn is that both the orbitals and the nuclei are arranged most compactly in the *gauche* rotamer. These results are in striking parallel with the arguments of Steiner [18] in connexion with the delocalization and contraction effects said to occur on conformational change.

The largest changes occurring in the orbital sizes on rotation are in the core and lone pair orbitals. Both increase considerably in radius (or volume) in the *trans* and *cis* rotamers, whilst the S–H orbital contracts somewhat in size. It seems surprising that the changes which take place in the *gauche* to *trans* rotation are almost, in total, twice those which occur in the change from *gauche-* to *cis*-HSSH. However, this may be the result of larger interactions in the *trans* rotamer between lone pair and bonding orbitals on adjacent sulphur centres, due to the shorter S–S bond.

4. Discussion

4.1. Rotational Barrier Analysis

Since the *gauche* rotamer is the most stable, HSSH has two rotational barriers. Experiment indicates [15] that, as anticipated, the *cis* barrier is higher than the *trans*, and that the sizes of the energy differences are considerably greater than in HOOH. The breakdown of the calculated total molecular energies into constituent parts given in Table 1 shows that both the electron–electron and nucleus–nucleus repulsions are *greatest* in the lowest energy rotamer, and vice versa. Naturally, as mentioned earlier, this is offset by the larger nucleus–electron attraction energy to be found in the most compact (gauche) structure. Indeed, there is good reason to suppose that a similar balance between the attractive and repulsive energies will always be followed, as a consequence of the Virial Theorem [18] and other considerations [29]. This being so, it remains to the theory to account for the considerable differences between the electronic energies of the rotamers (that is, excluding the nucleus–nucleus repulsion energy, which should always follow the same trend), rather than the very small difference in total energy. Even if there are exceptions, which would be unusually interesting to investigate, the present HSSH system is certainly accommodated within this scheme. The re-optimization of the geometry of each rotamer is therefore necessary before changes in the parts of the energy can be discussed, because the use of a standard geometry will not usually give a physically realistic balance between the energies [16–18, 29].

The distribution of the changes in the partitioned energies is given in histogram form in Fig. 4. This suggests that the "mechanism" of each rotational barrier may have a similar origin, since the distributions are surprisingly close in shape. In order to discover how the various orbitals have been affected following rotation, a further breakdown is required. This may be achieved by a straightforward transformation of the nonorthogonal set of FGO's $\{G_i\}$ to produce a set of orthogonal functions, called "Löwdin orbitals" $\{L_i\}$ [17]. This transformation ensures that

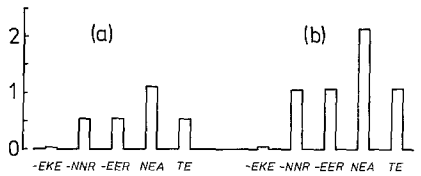

Fig. 4. Distribution of partitioned energy changes (a.u.) in (a) *gauche* to *trans* and (b) *gauche* to *cis* rotations

the orthonormal Löwdin orbitals are closest, in a least-squares sense, to the original FGO's [30]:

$$L_i = \sum_{k=1,n} S_{ki}^{-1/2} G_k \quad (S = \text{overlap matrix})$$

The transformation matrix is unitary, such that the total electronic energy is simply the sum of the average energy of each electron pair, $\varepsilon_{\text{pair}}$:

$$\varepsilon_{\text{pair}} = 2\langle L_i|h_1|L_i\rangle + \langle L_i L_i|h_2|L_i L_i\rangle + \sum_{j\neq i}^{n} (2\langle L_i L_i|h_2|L_j L_j\rangle - \langle L_i L_j|h_2|L_j L_i\rangle)$$

The first term represents the sum of the electronic kinetic (positive) and nucleus–electron attraction (negative) energies, the second (the "orbital self-repulsion" term) is the Coulomb repulsion between the two electrons in L_i and the summation gives the average electron–electron interaction (Coulomb and exchange) between a pair of electrons in L_i and the other electrons.

For the lone pairs, the equivalent orbitals produced by the sum and difference of the σ and π functions were used to calculate the necessary integrals.

These energy changes, in terms of the orbitals, are illustrated in Fig. 5. The total

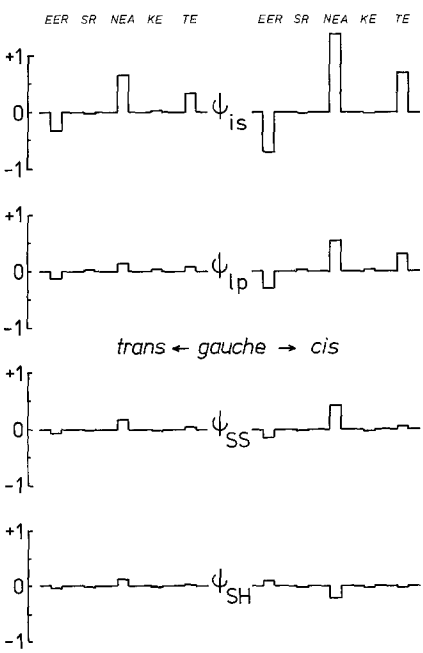

Fig. 5. Distribution of partitioned energy changes (a.u.) amongst the orbitals

electron pair energies (*TE*) increase on rotation either to the *cis* or *trans* conformer, except for the S–H bonding orbital in *cis*-HSSH, which becomes stabilized. This is probably due to the relative proximity of the protons opposite each S–H orbital. Rotation from *gauche* to *trans* produces greatest increase in the inner shell energies (62% of the total change). The S–S orbital contributes 20% to the changes in the electronic energy, whilst the lone pairs and S–H orbitals make up 12 and 7%, respectively, of the total change. Electronic energy changes which occur in the *gauche* → *cis* rotation are more evenly distributed amongst all the orbitals, although changes in the inner shell energies still account for just over half. These changes are significantly different from those obtained by Semkow and Linnett [17] for HOOH, in which the inner shell contribution was only 17%.

$\varepsilon_{\text{pair}}$(SS) increases by 0.7 and 1.3% on rotation from *gauche* to *trans* and from *gauche* to *cis*, respectively. The SS orbital is most affected energetically by the changes in conformation, and this may be ascribed (see Fig. 5) to the loss in nucleus–electron attraction energy in the expanded, higher energy rotamers. Although the total change in $\varepsilon_{\text{pair}}$ for the core orbitals is about three times the size of $\Delta\varepsilon_{\text{pair}}$(SS) in each case, these changes represent only 0.05 and 0.1% (*gauche* → *trans* and *gauche* → *cis*, respectively) of the total electronic energy of the inner shells. A hierarchy of the changes in the pair energies for each rotation may be constructed:

gauche → *trans* core : 1*p* : SS : SH = 1 : 2 : 14 : 3

gauche → *cis* core : 1*p* : SS : SH = 1 : 5 : 13 : 5

The analysis of the energy changes given above does not suggest why the lowest energy conformation is preferred over the others. Although $\varepsilon_{\text{pair}}$(SS) is most affected, this change could be the *result* of interactions between the orbitals in the two hydrosulphuryl parts of the molecule. However, since the S–S bond stretches appreciably on rotation, it might be expected that a correlation exists between, for example, the rotational barrier in HSSH and HOOH and the S–S and O–O bond strengths in these molecules. This does seem to be so: B(S–S) = 264 kJ mol^{-1}, B(O–O) = 142 kJ mol^{-1} [31] and R(*gauche* → *cis*) – HSSH 42 kJ mol^{-1} [15], HOOH 29 kJ mol^{-1} [32], R(*gauche* → *trans*) – HSSH 29 kJ mol^{-1} [15], HOOH 5 kJ mol^{-1} [32]. This correlation may well account for the importance of geometry optimization when predicting the rotational barriers in these particular molecules, especially HOOH [17]. Pappas also suggested [13] that the main effects of rotation around the S–S bond may be more concentrated in the S–S region than elsewhere.

Minyaev *et al.* proposed [33], from the results of several semiempirical calculations, that the rotational barriers in HSSH, HSeSeH and HTeTeH (but not HOOH) depended upon the interaction energy of the central atoms. The present FGO calculations on HSSH also indicate that the rotational energy differences are dominated by the inner shells, in contrast to similar FSGO calculations on HOOH [17].

VSEPR theory has been widely used to demonstrate how electron pair interactions

may be related to the shapes of molecules [20]. For rotational barriers, the use of the VSEPR model presents several difficulties, as Wolfe has pointed out [3], in connexion with the Gauche Effect. The main drawback to the model is that the sizes of the interactions between electron pairs are not given explicitly. For the HSSH system, Table 8 details the interactions between electron pairs across the

Table 8. VSEPR interactions in the HSSH system (a.u.)[a]

	trans	*gauche*	*cis*
a) Individual terms			
$L_{SH}/L_{S'H'}$	0.779786 (180°)	0.843120 (90°)	0.984460 (0°)
L_{SH}/L_{1p}	0.897654 (60°)	0.884803 (90°)[b]	0.849490 (120°)
$L_{1p}/L_{1p'}$	0.888179 (120°)[c]	0.903957 (90°)[d]	0.890677 (60°)[e]
b) Totals			
$L_{SH}/L_{S'H'}$	0.779786	0.843120	0.984460
L_{SH}/L_{1p}	3.590616	3.539212	3.397960
$L_{1p}/L_{1p'}$	3.552716	3.615826	3.562708
Total	7.923118	7.998158	7.945128

[a] For definition of VSEPR interaction, see text.
[b] Average of 0.825908 (150°) +0.943698 (30°).
[c] Average of 0.856552 (180°) +0.919806 (60°).
[d] Average of 0.902676 (90°, twice) +0.884930 (150°) +0.925544 (30°).
[e] Average of 0.857352 (120°) + 0.924002 (0°).

molecule for the three rotamers. The VSEPR interaction given in this table is the sum of the Coulomb and exchange integrals between an electron pair in orbital L_i and another in L_j, namely $2(2\langle L_iL_i|h_2|L_jL_j\rangle - \langle L_iL_j|h_2|L_jL_i\rangle)$. The results indicate that except for the *bp/bp* interaction, the other interactions between the orbitals change *irregularly* with dihedral angle. Clearly, the calculated values are not as expected from a straightforward application of VSEPR theory. It seems possible to advance three reasons for this discrepancy. Firstly, these interactions may not be the same as those required by the VSEPR model [20]. However, as observed in Sect. 3.1. (and Fig. 2), the interactions between the orbitals do follow the order required by the VSEPR model. Other wavefunctions have lead to similar results [34]. Secondly, as has been discussed by Wolfe [3], the proximity of lone pairs and polar bonds on adjacent centres, which characterizes the Gauche Effect, implies that an attraction may well be the primary interaction leading to gauche structures in molecules. Thirdly, it may be observed that the maximal value of the total electron–electron repulsion in the *gauche* rotamer, noted in previous discussion, leads to the result given in Table 8 that the total repulsion between the valence orbitals of the two halves of the molecule is also maximal for the *gauche* rotamer.

4.2. Gauche Effect in HSSH

The nature of the rotational barrier mechanism is clearly related to the Gauche Effect in the HSSH system. A straightforward application of the VSEPR approach

does not account for the observed order of stability amongst the rotamers. Therefore, it is necessary that any theoretical model must explain the lower energy of the gauche conformation.

Three slightly different approaches seem to have been employed. The first, due to Levitt and Levitt, involves a partial triple bond between the sulphurs [27]. The second, described by Wolfe, invokes an attraction between the lone pairs and polar S–H bonds [3], whilst the third, proposed by Radom, Hehre and Pople (RHP), requires the donation by a lone pair of π-symmetry on one centre into a partly vacant orbital on the other [35]. These approaches are clearly not mutually exclusive.

The triple bond description is supported by the population analysis (Table 6), which in turn is produced by the movement of $G_{S\pi}$ into a bonding position with respect to the S–S bond. This may be described as the attraction required by Wolfe's approach. The RHP description of the Gauche Effect utilizes the LCAO-MO model of molecular electronic structure. Since the gauche structure is correctly predicted to have the lowest energy by the present calculations, which do not formally include the partly vacant orbital able to accept electrons in this way, the RHP approach needs to be slightly generalized to accommodate the FGO results.

A complementary description of the extra binding in the gauche structure may be obtained by the construction of "General Symmetry Orbitals" (GSO's) for the rotamers in terms of the basis functions associated with the two SH units. Fig. 6

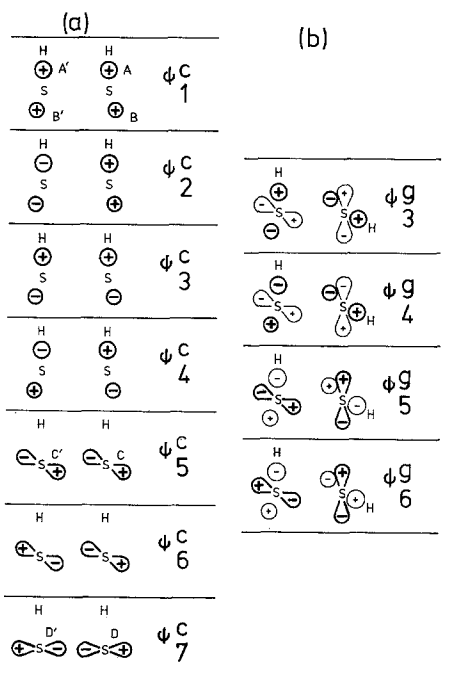

Fig. 6. Construction of General Symmetry Orbitals (a) in *cis*-HSSH (*trans*-HSSH has analogous combinations) and (b) mixing of ψ^{tc}_{3-6} in *gauche*-HSSH

illustrates how the orbitals may be combined to produce bonding and antibonding pairs which have additional stabilization in the gauche conformation. The lone pairs of π-symmetry mix with the opposite antisymmetric "*A–B*" combination giving mutually asymmetric charge distributions. The physical consequences suggested by this manifestation is that two pairs of "orbital dipoles" are produced in *gauche*-HSSH which, although having zero vector sum, have a negative (stabilizing) interaction energy. This leads to lower electron pair energies in the gauche structure for the lone pair orbitals of π-symmetry, a result which is born out by the SCF symmetry orbitals for the three rotamers. This approach, which involves the polarization of the GSO's in *gauche*-HSSH, is quite general. It may be applied to gauche conformations in other systems, whether or not these are symmetrical, for example CH_2F–OH [3].

References

1. Seel, F.: Advan. Inorg. Chem. Radiochem. **16**, 297 (1974)
2. Barnett, E. de B., Wilson, C. L.: Inorganic chemistry. London: Longmans 1959
3. Wolfe, S.: Accounts Chem. Res. **5**, 102 (1972)
4. Frost, A. A.: J. Chem. Phys. **47**, 3707 (1967)
5. Blustin, P. H., Linnett, J. W.: J. Chem. Soc. Faraday II **70**, 826 (1974)
6. Schwartz, M. E.: J. Chem. Phys. **51**, 4182 (1969)
7. Veillard, A., Demuynck, J.: Chem. Phys. Letters **4**, 476 (1969)
8. Hillier, I. H., Saunders, V. R., Wyatt, J. F.: Trans. Faraday Soc. **66**, 2665 (1970)
9. Christofferson, R. E., Nitzsche, L. E.: Computers for chemical research, Vol. 2. Amsterdam: Elsevier 1973
10. Boyd, D. B.: J. Phys. Chem. **78**, 1554 (1974)
11. Davies, D. W.: Chem. Phys. Letters **28**, 520 (1974)
12. Dixon, R. N., Hugo, J. M. V.: Mol. Phys. **29**, 953 (1975)
13. Pappas, J. A.: Chem. Phys. **12**, 397 (1976)
14. Winnewisser, G., Winnewisser, M., Gordy, W.: J. Chem. Phys. **49**, 3465 (1968)
15. Allinger, N. L., Hickey, M. J., Kao, J.: J. Am. Chem. Soc. **98**, 2741 (1976)
16. Blustin, P. H., Linnett, J. W.: J. Chem. Soc. Faraday II **70**, 290 (1974)
17. Semkow, A. M., Linnett, J. W.: J. Chem. Soc. Faraday II **71**, 1595 (1975)
18. Steiner, E.: The determination and interpretation of molecular wave functions. London: Cambridge University Press 1976
19. Blustin, P. H.: J. Chem. Phys.: **66**, 5648 (1977)
20. Gillespie, R. J.: J. Chem. Educ. **40**, 295 (1963)
21. Blustin, P. H.: unpublished results
22. Smith, C. P., Lewis, G. L., Grossman, A. J., Jennings, F. B.: J. Am. Chem. Soc. **62**, 1219 (1940)
23. Kaye, G. W. C., Laby, T. H.: Tables of physical and chemical constants. London: Longmans 1973
24. Amos, A. T., Crispin, R. J.: J. Chem. Phys. **63**, 4723 (1975)
25. Gregson, A. K.: Electronic structure and magnetism of inorganic compounds, Vol. 4. London: Chemical Society Specialist Periodical Reports 1976
26. Simons, G., Talaty, E. R.: Chem. Phys. Letters **38**, 422 (1976)
27. Levitt, L. S., Levitt, B. W.: Chem. Ind. (London) 132 (1973)
28. Blustin, P. H.: Chem. Phys. Letters **35**, 1 (1976)
29. Csizmadia, I. G., Theodorakopoulos, G., Schlegel, H. B., Whangbo, M.-H., Wolfe, S.: Can. J. Chem. **55**, 986 (1977)
30. Carlson, B. C., Keller, J. M.: Phys. Rev. **105**, 102 (1957)

31. Johnson, D. A.: Some thermodynamic aspects of inorganic chemistry. London: Cambridge University Press 1976
32. Pakiari, A. H., Linnett, J. W.: J. Chem. Soc. Faraday II **71**, 1590 (1975)
33. Minyaev, R. M., Minkin, V. I., Zakharov, I. I., Sadekov, I. D.: Teor. Eksp. Khim. **9**, 816 (1973), from Chem. Abstr. **80**, 70102k
34. Wilson, S., Gerratt, J.: Mol. Phys. **30**, 789 (1975)
35. Radom, L., Hehre, W. J., Pople, J. A.: J. Am. Chem. Soc. **94**, 2371 (1972)

Received November 14, 1977